



On a superconvergent lattice Boltzmann boundary scheme[☆]

François Dubois^{a,b,*}, Pierre Lallemand^c, Mahdi Tekitek^{a,1}

^a Numerical Analysis and Partial Differential Equations, Department of Mathematics, Paris Sud University, Orsay, France

^b Conservatoire National des Arts et Métiers, EA3196, Paris, France

^c Centre National de la Recherche Scientifique, Paris, France

ARTICLE INFO

Keywords:

Lattice Boltzmann scheme
Boundary conditions
Taylor expansion method

ABSTRACT

In a seminal paper [20], Ginzburg and Adler (1994) analyzed the bounce-back boundary conditions for the lattice Boltzmann scheme and showed that it could be made exact to second order for the Poiseuille flow if some expressions depending upon the parameters of the method were satisfied, thus defining so-called “magic parameters”. Using the Taylor expansion method that one of us developed, we analyze a series of simple situations (1D and 2D) for diffusion and for linear fluid problems using bounce-back and “anti bounce-back” numerical boundary conditions. The result is that “magic parameters” depend upon the detailed choice of the moments and of their equilibrium values. They may also depend upon the way the flow is driven.

© 2009 Elsevier Ltd. All rights reserved.

1. Introduction

The theoretical analysis of the lattice Boltzmann scheme [1–7] is an active subject of research. Recall that the method was first analyzed by d’Humières [5] with a Chapman–Enskog expansion coming from statistical physics; we also refer to Asinari and Ohwada [8] for a method of analysis based on the Grad moment system. A fruitful idea followed by Junk et al. [9–11] is to use the so-called equivalent equation method derived independently by Lerat–Peyret [12] and Warming and Hyett [13] (see also [14]). An infinitesimal parameter is introduced and the finite differences operators are expanded into a family of equivalent partial differential equations. The main goal of this study is to use the Taylor expansion method [10,11] in order to increase the accuracy of boundary conditions for simple problems with analytical solutions. We first consider a one-dimensional (1D) diffusion problem and study the influence of the definition of the moments and of their equilibrium value. We then consider a two-dimensional (2D) Poiseuille flow using several ways to enforce a pressure gradient.

We consider regular lattices parametrized by a space step Δx . We introduce a time step Δt and adopt “acoustic” scaling: the ratio $\lambda \equiv \frac{\Delta x}{\Delta t}$ is a **fixed** reference velocity for each study. As a consequence, the parameters Δx and Δt are equivalent infinitesimals. Note that as this work is devoted to boundaries, we shall use a particular way to test the accuracy of a numerical scheme as will be discussed later.

2. Diffusion problem in one space dimension

We consider the classical Lattice Boltzmann model D1Q3 with three discrete velocities and one conservation law to model diffusion problems. We choose the velocities v_i ($0 \leq i \leq 2$) such that $v_0 = 0$, $v_1 = \lambda$, $v_2 = -\lambda$. At each mesh point, there

[☆] Contribution presented at the fifth ICMMS Conference (Amsterdam, 16–20 June 2008).

* Corresponding author at: Numerical Analysis and Partial Differential Equations, Department of Mathematics, Paris Sud University, Orsay, France.
E-mail addresses: francois.dubois@math.u-psud.fr (F. Dubois), pierre.lal@free.fr (P. Lallemand), mohamed-mahdi.tekitek@math.u-psud.fr (M. Tekitek).

¹ Present address: Department of Mathematics, F.S.T., University El Manar, Tunis, Tunisia.

are three functions $\{f_j\}$ that can be interpreted as populations of fictitious particles. These populations evolve according to the lattice Boltzmann scheme which we write as in [10]:

$$f_j(x, t + \Delta t) = f_j^*(x - v_j \Delta t, t), \quad 0 \leq j \leq 2, \tag{1}$$

where the superscript $*$ denotes post-collision quantities and x a vertex of the lattice. Therefore during each time increment Δt there are two fundamental steps: advection and collision. The **advection** step describes the motion of a particle which has undergone collision at node $x - v_j \Delta t$ and goes to the j th neighboring node. Following d’Humières [5], the **collision** step is defined in the space of moments. For D1Q3 three moments $\{m_\ell\}$ are obtained by a linear transformation of vectors f_j :

$$m_0 = f_0 + f_1 + f_2 \equiv \rho(\text{density}), \quad m_1 = \lambda(f_1 - f_2), \quad m_2 = \frac{\lambda^2}{2}(f_1 + f_2). \tag{2}$$

In consequence, we introduce a matrix of moments M to represent moments like (2); it takes the form

$$M = \begin{pmatrix} 1 & 1 & 1 \\ 0 & \lambda & -\lambda \\ 0 & \frac{\lambda^2}{2} & \frac{\lambda^2}{2} \end{pmatrix} \tag{3}$$

and the relations (2) can be simply written as $m = Mf$. To simulate diffusion problems, we conserve only the density moment ρ in the collision step and obtain one macroscopic scalar equation. The other quantities (nonconserved moments) are assumed to relax towards equilibrium values (m_1^{eq}, m_2^{eq}) following:

$$m_\ell^* = (1 - s_\ell) m_\ell + s_\ell m_\ell^{eq}, \quad 1 \leq \ell \leq 2, \tag{4}$$

where s_ℓ ($0 < s_\ell < 2$, for $\ell = 1, 2$) are relaxation rates, not necessarily equal to a single value as in the BGK case [4]. The equilibrium values m_ℓ^{eq} of the nonconserved moments in Eq. (4) determine the macroscopic behavior of the scheme. Indeed with the following choice of equilibrium values (neglecting nonlinear contributions):

$$m_1^{eq} = 0, \quad m_2^{eq} = \zeta \frac{\lambda^2}{2} \rho \tag{5}$$

and using the Taylor expansion method we find (see e.g. [15]) that the equivalent partial differential equation of the numerical scheme up to order three in Δx is a diffusion equation:

$$\frac{\partial \rho}{\partial t} - \kappa \frac{\partial^2 \rho}{\partial x^2} = O(\sigma_1 \Delta x^3). \tag{6}$$

The value of the diffusivity κ is given according to

$$\kappa = \Delta t \lambda^2 \sigma_1 \zeta \tag{7}$$

where $\sigma_\ell \equiv \frac{1}{s_\ell} - \frac{1}{2}$, $\ell = 1, 2$.

Remark that the thermal diffusivity κ is imposed by the Physics. Moreover the scale velocity λ is fixed and the coefficient ζ is also imposed. When we refine the mesh, the coefficient σ_1 must be chosen in order to enforce relation (7). In other terms, the product $\sigma_1 \Delta t$ must be maintained constant. Then the right hand side of relation (6) exhibits a **second order truncation error** of the lattice Boltzmann scheme for a **given** thermal diffusivity κ . Associated with stability properties (see Junk and Yong [16]), convergence properties of lattice Boltzmann scheme can be established, as in [17].

3. Localization of a 1D boundary

Let us introduce a constant c and consider the following 1D Poisson problem:

$$-\mathbf{K} \frac{d^2 \rho}{dx^2} = c \quad \text{in }]0, 1[, \quad \rho(0) = \rho(1) = 0. \tag{8}$$

We take an “anti bounce-back” numerical boundary condition at $x = 0$:

$$f_1(x_b, t + \Delta t) = -f_2(x_e, t + \Delta t) = -f_2^*(x_b, t), \tag{9}$$

with x_b the fluid node and x_e the external node as presented in Fig. 1, and a similar condition for $x = 1$. A uniform body source (δp) is added to the Boltzmann scheme to model the right hand side c of Eq. (8). So we can write the lattice Boltzmann scheme as follows: (i) $m = Mf$, (ii) $\tilde{m}_0 = m_0 + \frac{1}{2} \delta p$, (iii) evaluate the other moments, (iv) relaxation (4) of the other moments, (v) $\tilde{m}_0 = m_0 + \frac{1}{2} \delta p$, (vi) $f = M^{-1}m$, (vii) advection step (1) and boundary conditions. The exact solution of problem (8) is elementary: $u(x) = \frac{cx(1-x)}{2K}$. We analyze the behavior of the discrete model to show whether it can be tuned so that the location of the “numerical boundary” can be fixed at mid-point as expected from “anti bounce-back”. Thus we shall use as criterion for accuracy the difference between the imposed boundary and the “numerically determined” boundary.

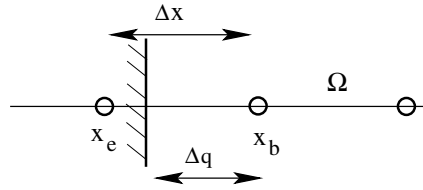


Fig. 1. A boundary surface cutting the link between a fluid node x_b and a fictitious outside node $x_e \equiv x_b - \Delta x$.

From a theoretical point of view, we suppose that the discrete fields $f_j(x, t)$ vary slowly in space and time in order to be able to use Taylor expansions. We analyze the lattice Boltzmann scheme in terms of equivalent partial differential equations and formal developments. It is well known (see e.g. Griffiths and Sanz-Serna [18] or Chang [19]) that this method of analysis fails *a priori* to predict boundary effects properly if this hypothesis is not satisfied. We keep in mind this restriction in our numerical experiments. Nevertheless, this elementary tool can produce nontrivial results, as we will see hereafter.

We say in the following that a boundary scheme (such as (9) to fix the ideas) is of order p at location Δq relative to homogeneous Dirichlet boundary condition (that are present in (8)) if the numerical boundary condition implies

$$\rho(x_b - \Delta q) = O(\Delta x^p) \tag{10}$$

for the continuous conserved field issued from the particle field $f_j(x, t)$ according to (2). We have the following result:

Proposition 1. For the D1Q3 lattice Boltzmann scheme (1) (2) (4) (5), the “anti bounce-back” numerical boundary condition (9) is of order 3 at location $\Delta q = \frac{\Delta x}{2}$ relative to the homogeneous Dirichlet boundary condition of problem (8) if and only if the following condition

$$\sigma_1 \sigma_2 = \frac{1}{8} \tag{11}$$

is satisfied.

Relation (11) defines superconvergent parameters σ_1 and σ_2 . Recall that they have been called “magic” by I. Ginzbourg and P.M. Alder [20].

Proof. We have introduced in [10,11] the “tensor of momentum velocities” and the so-called “defects of conservation” which are defined respectively by

$$\begin{aligned} \Lambda_{k\alpha}^\ell &\equiv \sum_j M_{kj} M_{\alpha j} (M^{-1})_{j\ell} \\ \theta_k &\equiv \partial_t m_k^{eq} + \Lambda_{k\alpha}^\ell \partial_\alpha m_\ell^{eq}, \quad k \geq 1. \end{aligned} \tag{12}$$

For the D1Q3 lattice Boltzmann scheme applied to diffusion problem like (8),

$$\theta_1 = \zeta \lambda^2 \frac{\partial \rho}{\partial x}, \quad \theta_2 = \zeta \frac{\lambda^2}{2} \frac{\partial \rho}{\partial t}. \tag{13}$$

Then we obtain the following development of nonequilibrium moments at third order (as described in [15]):

$$m_k^* = m_k^{eq} + \Delta t \left(\frac{1}{2} - \sigma_k \right) [\theta_k - \Delta t (\sigma_k \partial_t \theta_k + \sigma_\ell \Lambda_{k\alpha}^\ell \partial_\alpha \theta_\ell)] + O(\Delta x^3), \quad k \geq 1. \tag{14}$$

Thus for $k = 1$:

$$m_1^* = \Delta t \left(\frac{1}{2} - \sigma_1 \right) [\theta_1 - \Delta t (\sigma_1 \partial_t \theta_1 + \sigma_1 \Lambda_{11}^1 \partial_x \theta_1 + \sigma_2 \Lambda_{11}^2 \partial_x \theta_2)] + O(\Delta x^3).$$

Using (13) and $\partial_t \theta_1 = O(\Delta t^2)$, $\Lambda_{11}^1 = 0$ the above equation becomes:

$$m_1^* = \Delta t \lambda^2 \left(\frac{1}{2} - \sigma_1 \right) \zeta \frac{\partial \rho}{\partial x} + O(\Delta x^3). \tag{15}$$

For $k = 2$, we use expression (5) of m_2^{eq} , together with $\theta_2 = 0$ and $\Lambda_{21}^1 = \frac{\lambda^2}{2}$ to obtain from (14):

$$m_2^* = \lambda^2 \frac{\zeta}{2} \rho - \Delta t^2 \lambda^4 \frac{\zeta}{2} \sigma_1 \left(\frac{1}{2} - \sigma_2 \right) \frac{\partial^2 \rho}{\partial x^2} + O(\Delta x^3) \tag{16}$$

Using the inverse moment matrix M^{-1} , the post-collision f are given by:

$$f_1^* = \frac{1}{2\lambda^2} [2m_2^* + \lambda m_1^*], \quad f_2^* = \frac{1}{2\lambda^2} [2m_2^* - \lambda m_1^*]. \tag{17}$$

At the boundary, due to (1) and (9), we consider the following quantity:

$$f_1^*(x_e) + f_2^*(x_b) = \frac{1}{2\lambda^2} [2(m_2^*(x_e) + m_2^*(x_b)) + \lambda(m_1^*(x_e) - m_1^*(x_b))]. \tag{18}$$

Using relations (16) and (15) we obtain respectively:

$$\begin{cases} m_2^*(x_e) + m_2^*(x_b) = \lambda^2 \frac{\zeta}{2} [\rho(x_e) + \rho(x_b)] \\ -\Delta t^2 \lambda^4 \frac{\zeta}{2} \sigma_1 \left(\frac{1}{2} - \sigma_2 \right) \left[\frac{\partial^2 \rho}{\partial x^2}(x_e) + \frac{\partial^2 \rho}{\partial x^2}(x_b) \right] + O(\Delta x^3) \end{cases} \tag{19}$$

$$m_1^*(x_e) - m_1^*(x_b) = \Delta t \lambda^2 \zeta \left(\frac{1}{2} - \sigma_1 \right) \left[\frac{\partial \rho}{\partial x}(x_e) - \frac{\partial \rho}{\partial x}(x_b) \right] + O(\Delta x^3). \tag{20}$$

With the help of classical Taylor expansion we have, with the notation $x_i \equiv \frac{1}{2}(x_b + x_e)$:

$$\rho(x_e) + \rho(x_b) = 2\rho(x_i) + \frac{\Delta x^2}{4} \frac{\partial^2 \rho}{\partial x^2}(x_i) + O(\Delta x^3), \tag{21}$$

$$\frac{\partial \rho}{\partial x}(x_e) - \frac{\partial \rho}{\partial x}(x_b) = -\Delta x \frac{\partial^2 \rho}{\partial x^2}(x_i) + O(\Delta x^3), \tag{22}$$

$$\frac{\partial^2 \rho}{\partial x^2}(x_e) + \frac{\partial^2 \rho}{\partial x^2}(x_b) = 2 \frac{\partial^2 \rho}{\partial x^2}(x_i) + O(\Delta x^2). \tag{23}$$

Considering Eq. (18), together with (19), (20) and taking into account relations (21), (22) and (23) we obtain:

$$f_1^*(x_e) + f_2^*(x_b) = \zeta \rho(x_i) + \zeta \Delta x^2 \left(\sigma_1 \sigma_2 - \frac{1}{8} \right) \frac{\partial^2 \rho}{\partial x^2}(x_i) + O(\Delta x^3). \tag{24}$$

Due to the simple fundamental expression (1) of a lattice Boltzmann scheme, the left hand side of (24) is identically null when the numerical boundary condition (9) occurs. Due to the relation $x_i = \frac{1}{2}(x_b + x_e)$, the condition (10) is satisfied with $\Delta q = \frac{\Delta x}{2}$ and $p = 3$ if and only if $\sigma_1 \sigma_2 = \frac{1}{8}$. \square

• Let us now consider the effect of using a **different** moment matrix for the D1Q3 case:

$$M = \begin{pmatrix} 1 & 1 & 1 \\ 0 & \lambda & -\lambda \\ -2\lambda^2 & \lambda^2 & \lambda^2 \end{pmatrix}. \tag{25}$$

obtained from (3) by a Gram–Schmidt orthogonalization algorithm as usual with the lattice Boltzmann scheme (see e.g. [7]). The moments at equilibrium are now given by $m_1^{eq} = 0$ and $m_2^{eq} = \lambda^2 \zeta \rho$. We remark that the matrix of moments (25) leads to an equivalent macroscopic conservation law of type (6) with a diffusivity κ which is now given by $\kappa = \Delta t \lambda^2 \sigma_1 \frac{2+\zeta}{3}$.

Proposition 2. *The D1Q3 lattice Boltzmann scheme (1) (25) (4) (5) associated to the “anti bounce-back” numerical boundary condition (9) is of order 3 at location $\Delta q = \frac{\Delta x}{2}$ for the homogeneous Dirichlet boundary condition of problem (8) if and only if $\sigma_1 \sigma_2 = \frac{3}{8}$.*

Remark that the superconvergent parameters satisfying the relation (11) emerging from Proposition 1 with the choice of transformation matrix M given by (3) are **different** from those obtained in the case with matrix (25).

Proof. For this model we have the following Taylor development of nonconserved moments up to order 2 on Δx :

$$\begin{aligned} m_1^* &= \Delta t \lambda^2 \left(\frac{1}{2} - \sigma_1 \right) \left(\frac{2+\zeta}{3} \right) \frac{\partial \rho}{\partial x} + O(\Delta x^3), \\ m_2^* &= \lambda^2 \zeta \rho - \Delta t^2 \lambda^4 \sigma_1 \left(\frac{1}{2} - \sigma_2 \right) \left(\frac{2+\zeta}{3} \right) \frac{\partial^2 \rho}{\partial x^2} + O(\Delta x^3). \end{aligned}$$

With the help of the matrix moments (25) we have:

$$f_1^* = \frac{1}{3} \rho + \frac{1}{6\lambda^2} [m_2^* + 3\lambda m_1^*], \quad f_2^* = \frac{1}{3} \rho + \frac{1}{6\lambda^2} [m_2^* - 3\lambda m_1^*].$$

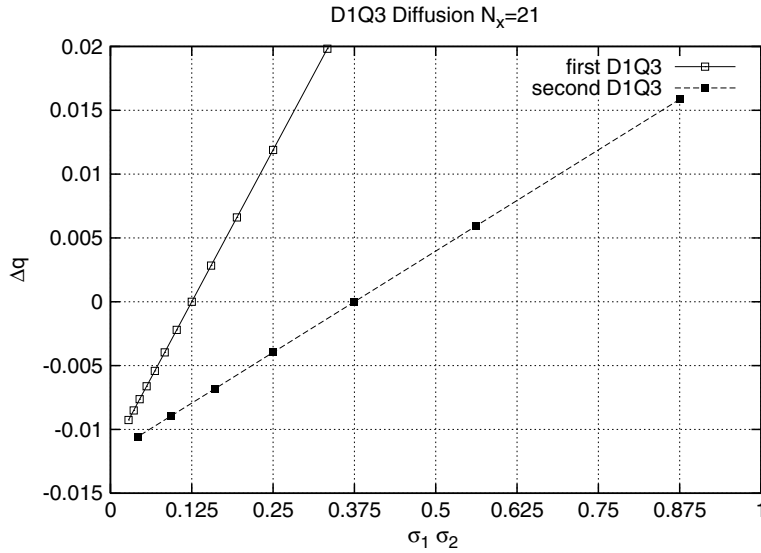


Fig. 2. “Experimental numerical location” of the solid wall Δq versus $\sigma_1 \sigma_2$. The first D1Q3 model with \square symbol: superconvergent parameters such that $\sigma_1 \sigma_2 = \frac{1}{8}$. The second D1Q3 model with \blacksquare symbol: superconvergent parameters satisfying $\sigma_1 \sigma_2 = \frac{3}{8}$.

As $f_2(x_b)$ is internal to the domain we add to $\rho(x_b)$ a body source $\delta\rho = -\frac{2+\tilde{\zeta}}{3} \frac{\partial^2 \rho}{\partial x^2}$. Now by using the same method as in the proof of Proposition 1, we obtain:

$$f_1^*(x_e) + f_2^*(x_b) = \frac{2 + \tilde{\zeta}}{3} \rho(x_i) + \Delta x^2 (8\sigma_1 \sigma_2 - 3) \frac{2 + \tilde{\zeta}}{72} \frac{\partial^2 \rho}{\partial x^2}(x_i) + O(\Delta x^3).$$

The conclusion is a direct consequence of the above calculus. \square

To illustrate the preceding discussion, we perform a numerical simulation of the two lattice Boltzmann models and analyze (after a suitable number of iterations to reach steady state) the “Poiseuille” parabolic profile. We measure the numerical error in terms of a precise location of the boundary for Dirichlet type boundary condition. We follow a method proposed by Ginzburg and d’Humières [21]: from the numerical discrete field $u_{iB}(j\Delta x)$ we determine by least squares a parabola that fit at best the data. Then we calculate where this approximation of the numerical solution u_{iB} is equal to zero. We interpret this location as the “experimental numerical location” of the solid wall. We find **experimentally** that the extrapolated location of the Dirichlet boundary condition is located between x_b and x_e and this exact solid wall location is parametrized under the form $x_b - \Delta q$, with $0 \leq \Delta q \leq \Delta x$. The results obtained for several values of σ_1 and σ_2 are shown in Fig. 2 to depend only upon the product $\sigma_1 \sigma_2$ and go through 0 respectively for $\frac{1}{8}$ or $\frac{3}{8}$, in **complete coherence** with the Taylor expansion method developed in Propositions 1 and 2.

4. The 2D Poiseuille flow

We consider here the classical D2Q9 model (see e.g. [7]). We study a Poiseuille flow (in linear regime), first with an imposed uniform body force and periodic boundary condition at the inlet and outlet of the channel. Then we consider the same flow with an imposed difference of pressure between inlet and outlet. The evolution of the lattice Boltzmann scheme is given by Eq. (1). The corresponding moments have an explicit physical significance: $m_0 \equiv \rho$ is the density, $m_1 \equiv j_x$ and $m_2 \equiv j_y$ are x and y components of momentum, m_3 is the energy, m_4 is related to square energy, m_5, m_6 are x and y components of heat flux and m_7, m_8 are diagonal stress and off-diagonal stress. A Gram–Schmidt orthogonalization method is also used and the matrix of moments is exactly that used in [10,7]. The collision is described in the moments space as:

$$m_\ell^* = (1 - s_\ell)m_\ell + s_\ell m_\ell^{eq}, \quad 3 \leq \ell \leq 8, \tag{26}$$

where the equilibrium values m_k^{eq} are given by:

$$m_3^{eq} = \alpha\rho, \quad m_4^{eq} = \beta\rho, \quad m_5^{eq} = -\frac{j_x}{\lambda}, \quad m_6^{eq} = -\frac{j_y}{\lambda}, \quad m_7^{eq} = 0, \quad m_8^{eq} = 0. \tag{27}$$

• *The Poiseuille flow*

We introduce a 2D domain $\Omega =]0, L[\times]0, H[$ (see Fig. 3). Let $\mathbf{u}(t, x, y) \equiv (u, v)$ be the velocity of fluid and p the pressure solution of the “Poiseuille”–Stokes system:

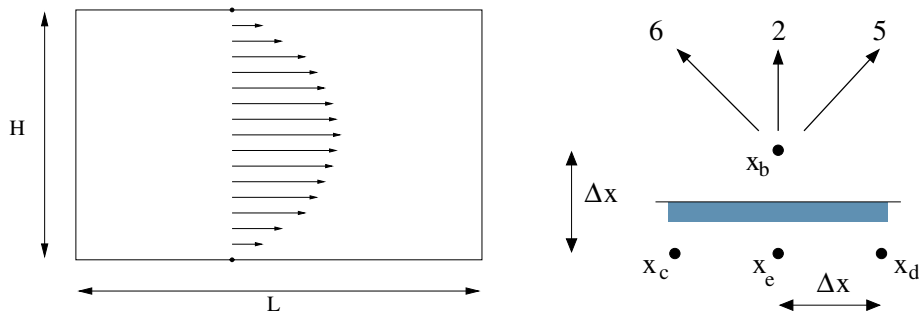


Fig. 3. Domain $\Omega =]0, L[\times]0, H[$ (left) and notations for the numerical treatment of a boundary vertex x_b at the bottom of domain Ω (right).

$$-\nu \Delta \mathbf{u} + \frac{1}{\rho} \nabla p = 0, \quad \text{div } \mathbf{u} = 0 \quad \text{in } \Omega \tag{28}$$

with the following boundary conditions:

$$p(0, y) = -p(L, y) = \delta p \quad \text{for } 0 \leq y \leq H, \quad \mathbf{u}(x, 0) = \mathbf{u}(x, H) = 0 \quad \text{for } 0 \leq x \leq L. \tag{29}$$

The solution of the above problem is classical: $\mathbf{u}(x, y) \equiv (u(y) = K y(H - y), v = 0)$, $p(x, y) = 2\rho\nu K x + P_0$, where P_0 is a given constant. We note that the problem (28) (29) is equivalent to a flow resulting from the action of a constant external force \mathbf{F} between two parallel walls with periodic boundary conditions on the inlet and the outlet of the channel (i.e. in the Ox direction). So the problem (28) (29) becomes:

$$-\nu \Delta \mathbf{u} = \mathbf{F}, \quad \mathbf{u}(x, 0) = \mathbf{u}(x, H) = 0, \tag{30}$$

where $\mathbf{F} = (F_x, 0)$ is the external force. The solution is given by $\mathbf{u}(x, y) = (u(y) = \frac{F_x}{2\nu} y(H - y), v = 0)$.

• A first lattice Boltzmann scheme

We use the D2Q9 lattice Boltzmann scheme to model the Poiseuille flow described by Eq. (30). We use the equilibrium (27) with $s_7 = s_8 = \left(\frac{1}{2} + \frac{3v}{\lambda^2 \Delta t}\right)^{-1}$ to have the exact viscosity ν present in Eq. (30). The implementation of the lattice Boltzmann scheme is conducted as follows for an arbitrary mesh vertex x of the lattice.

At initial time step $t = t_0$ we set the vectors $f(x, t_0) = 0$. For any given time t , we first determine the moments m_k using the relation $m \equiv Mf$. Then we change velocity j_x before the collision step by adding a half of the external force F_x : $j_x = j_x + \frac{\Delta t}{2} F_x$. Thus the macroscopic moments (density and velocity) are evaluated. Then we perform the collision step in moments space according to relation (26) and we add half of the external force F_x to the conserved velocity \tilde{j}_x : $j_x(t + \Delta t) = \tilde{j}_x + \frac{\Delta t}{2} F_x$. Using the matrix M^{-1} we compute the particle distributions $f_\alpha^*(x, t)$. We perform advection through a relation analogous to (1) and we obtain the vector $f_\alpha(x + v_\alpha \Delta t, t + \Delta t)$ for $0 \leq \alpha \leq 8$, if $x + v_\alpha \Delta t$ is a lattice node. For a boundary node as x_b of Fig. 3, we use (with the usual numbering of the degrees of freedom for D2Q9 scheme [7]) the following bounce-back boundary condition

$$\begin{cases} f_2(x_b, t + \Delta t) = f_4(x_e, t + \Delta t) = f_4^*(x_b, t) \\ f_5(x_b, t + \Delta t) = f_7(x_c, t + \Delta t) = f_7^*(x_b, t) \\ f_6(x_b, t + \Delta t) = f_8(x_d, t + \Delta t) = f_8^*(x_b, t). \end{cases} \tag{31}$$

Periodic boundary conditions are considered in the longitudinal direction for abscissas equal to 0 and L . We repeat those steps until convergence to a steady state.

Proposition 3. For the D2Q9 lattice Boltzmann scheme (1) (26) (27) the bounce-back numerical boundary condition (31) is of order 3 at location $\Delta q = \frac{\Delta x}{2}$ for the Dirichlet boundary condition $\mathbf{u} = 0$ if and only if $\sigma_5 \sigma_8 = \frac{3}{8}$.

Proof. We calculate the defects of conservation θ_k defined by (12) for $k > 3$:

$$\begin{aligned} \theta_3 &= \partial_t(\alpha\rho) = -\alpha \text{div } j + O(\Delta x^2), & \theta_4 &= \partial_t(\beta\rho) - \text{div } j = -(\beta + 1) \text{div } j + O(\Delta x^2), \\ \theta_5 &= -\frac{\partial j_x}{\lambda} + \frac{\lambda(\alpha + \beta)}{3} \partial_x \rho = \frac{\lambda}{6} (4 + 3\alpha + 2\beta) \partial_x \rho + O(\Delta x), \\ \theta_6 &= -\frac{\partial j_y}{\lambda} + \frac{\lambda(\alpha + \beta)}{3} \partial_y \rho = \frac{\lambda}{6} (4 + 3\alpha + 2\beta) \partial_y \rho + O(\Delta x), \\ \theta_7 &= \frac{2}{3} (\partial_x j_x - \partial_y j_y) & \theta_8 &= \frac{1}{3} (\partial_y j_x + \partial_x j_y). \end{aligned}$$

Nonequilibrium moments at second order are given by the expansion (14) (justified in [15,22]). Then we have:

$$\begin{aligned}
 m_3^* &= \alpha \rho + \Delta t \left(\frac{1}{2} - \sigma_3 \right) \left[-\alpha \operatorname{div} j + \Delta t \frac{\lambda^2}{6} (\sigma_3 \alpha (4 + \alpha) + \sigma_5 (4 + 3\alpha + 2\beta)) \Delta \rho \right] + O(\Delta x^3), \\
 m_4^* &= \beta \rho + \Delta t \left(\frac{1}{2} - \sigma_4 \right) \left[-(\beta + 1) \operatorname{div} j + \Delta t \frac{\lambda^2}{6} (\sigma_4 (\beta + 1) (4 + \alpha) + \sigma_5 (4 + 3\alpha + 2\beta)) \Delta \rho \right] + O(\Delta x^3), \\
 m_5^* &= -\frac{j_x}{\lambda} + \Delta t \left(\frac{1}{2} - \sigma_5 \right) \left[\lambda \frac{(4 + 3\alpha + 2\beta)}{6} \partial_x \rho + \Delta t \frac{\lambda}{3} \left(\frac{(4 + 3\alpha + 2\beta)}{2} \sigma_5 \partial_x \operatorname{div} j \right. \right. \\
 &\quad \left. \left. + \alpha \sigma_3 \partial_x \operatorname{div} j + (\beta + 1) \sigma_4 \partial_x \operatorname{div} j + 2\sigma_8 \partial_x (\partial_x j_x - \partial_y j_y) - \sigma_8 \partial_y (\partial_y j_x + \partial_x j_y) \right) \right] + O(\Delta x^3), \\
 m_6^* &= -\frac{j_y}{\lambda} + \Delta t \left(\frac{1}{2} - \sigma_5 \right) \left[\lambda \frac{(4 + 3\alpha + 2\beta)}{6} \partial_y \rho + \Delta t \frac{\lambda}{3} \left(\frac{(4 + 3\alpha + 2\beta)}{2} \sigma_5 \partial_y \operatorname{div} j \right. \right. \\
 &\quad \left. \left. + \alpha \sigma_3 \partial_y \operatorname{div} j + (\beta + 1) \sigma_4 \partial_y \operatorname{div} j - 2\sigma_8 \partial_y (\partial_x j_x - \partial_y j_y) - \sigma_8 \partial_x (\partial_y j_x + \partial_x j_y) \right) \right] + O(\Delta x^3), \\
 m_7^* &= \Delta t \left(\frac{1}{2} - \sigma_8 \right) \left[\frac{2}{3} (\partial_x j_x - \partial_y j_y) + \Delta t \frac{\lambda^2}{9} \left(\sigma_8 (4 + \alpha) + \frac{\sigma_5}{2} (4 + 3\alpha + 2\beta) \right) (\partial_x^2 \rho - \partial_y^2 \rho) \right] + O(\Delta x^3), \\
 m_8^* &= \Delta t \left(\frac{1}{2} - \sigma_8 \right) \left[\frac{1}{3} (\partial_y j_x + \partial_x j_y) + \Delta t \frac{\lambda^2}{9} (\sigma_8 (4 + \alpha) - \sigma_5 (4 + 3\alpha + 2\beta)) \partial_{xy} \rho \right] + O(\Delta x^3).
 \end{aligned}$$

We have $j_y = 0, j_x = j_{x0} + y \partial_y j_x + \frac{y^2}{2} \partial_y^2 j_x$ and $\rho = \text{constant}$. We evaluate the nonconserved moments $m_k^*(x_b)$ and add $m_1(x_b) = j_x(x_b) = j_x(x_i) + \frac{\Delta x^2}{3} \sigma_8 \partial_y^2 j_x(x_i) + O(\Delta x^3)$. We compute moments $m_k^*(x_e), m_k^*(x_c)$ and $m_k^*(x_d)$ at the “external nodes” depicted in Fig. 3. Using the matrix M^{-1} we evaluate $f_k^*(x_b), f_k^*(x_c), f_k^*(x_d)$ and $f_k^*(x_e)$. Finally we obtain

$$f_5^*(x_c) - f_7^*(x_b) = \frac{1}{6} j_x(x_i) + \frac{\Delta x^2}{144} (8\sigma_5 \sigma_8 - 3) \frac{\partial^2 j_x}{\partial y^2}(x_i) + O(\Delta x^3) \tag{32}$$

and similar relations for $f_2^*(x_e) - f_4^*(x_b)$ and $f_6^*(x_d) - f_8^*(x_b)$. The conclusion is clear: when the left hand side of (32) is identically null due to the boundary condition (31), the momentum $j_x(x_i)$ on the surface located at $\Delta q = \frac{1}{2} \Delta x$ is null “up to third order accuracy” as defined in (10) if and only if the relation $8\sigma_5 \sigma_8 - 3 = 0$ occurs. □

We remark that if we apply the body force following the algorithm (i) $m = Mf$, (ii) collision, (iii) $f = M^{-1}m$, (iv) apply the body force following the precise relations for transformation of particle distribution $f \rightarrow f: f_1 = f_1 + \frac{F_x}{3\lambda}, f_2 = f_2, f_3 = f_3 - \frac{F_x}{3\lambda}, \tilde{f}_4 = f_4, \tilde{f}_5 = f_5 + \frac{F_x}{12\lambda}, \tilde{f}_6 = f_6 - \frac{F_x}{12\lambda}, \tilde{f}_7 = f_7 - \frac{F_x}{12\lambda}, \tilde{f}_8 = f_8 + \frac{F_x}{12\lambda}$, which are equivalent in moments space to $\tilde{j}_x = j_x + F_x, \tilde{m}_5 = m_5 - \frac{F_x}{\lambda}$ and $\tilde{m}_k = m_k$ for the other moments, the solid wall for the Poiseuille problem is “numerically located” at $\Delta q = \frac{\Delta x}{2}$ up to third order accuracy if the relation $\sigma_5 \sigma_8 = \frac{3}{16}$ is satisfied between the relaxation parameters, as proposed by Ginzburg and d’Humières [23–25].

• A second lattice Boltzmann scheme

We can also model the Poiseuille flow described by (28) (29) with the explicit introduction of a pressure gradient δp . So the scheme (26) (27) has the same steps as the preceding scheme with $F_x \equiv 0$ and the wall boundary conditions are still given by (31). We consider the boundary condition for nodes $x \equiv (k\Delta x, \ell\Delta x)$ at the entrance ($k = 1$) and at the output ($k = N_x$) as follows:

$$\begin{cases}
 f_1(1, \ell) = -f_3(0, \ell) + \frac{1}{18} (4 - \alpha - 2\beta) \delta \rho, \\
 f_5(1, \ell) = -f_7(0, \ell - 1) + \frac{1}{18} (4 - \alpha - 2\beta) \delta \rho, \\
 f_8(1, \ell) = -f_6(0, \ell + 1) + \frac{1}{18} (4 - \alpha - 2\beta) \delta \rho, \\
 f_3(N_x, \ell) = -f_1(N_x + 1, \ell) - \frac{1}{18} (4 - \alpha - 2\beta) \delta \rho, \\
 f_6(N_x, \ell) = -f_8(N_x + 1, \ell - 1) - \frac{1}{18} (4 - \alpha - 2\beta) \delta \rho, \\
 f_7(N_x, \ell) = -f_5(N_x + 1, \ell + 1) - \frac{1}{18} (4 - \alpha - 2\beta) \delta \rho,
 \end{cases} \tag{33}$$

with $\delta \rho = \delta p / c_s^2$ the density drop corresponding to the pressure step considered in (29), (c_s is the speed of sound) and (α, β) parameters for equilibrium introduced at the relation (27). Note that these expressions may be called “anti bounce-back” with an imposed scalar quantity (similar to what is used when the lattice Boltzmann scheme is set to simulate diffusion problems).

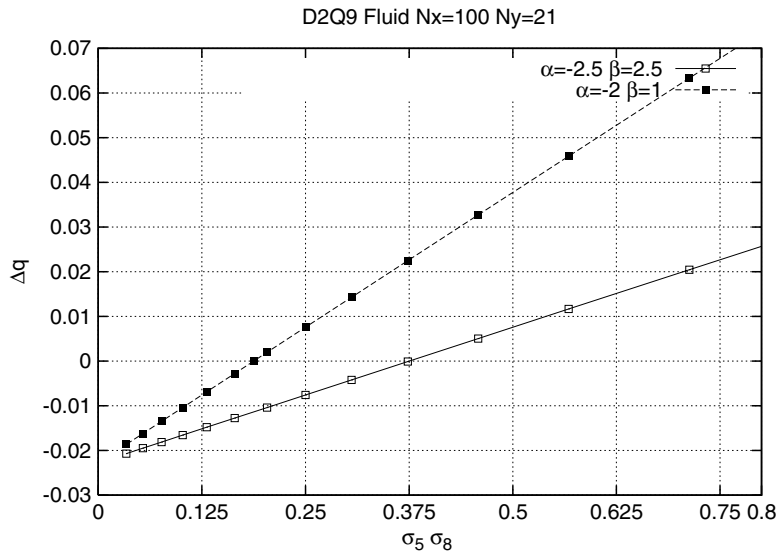


Fig. 4. Product $\sigma_5\sigma_8$ versus solid wall location Δq with $N_y = 21$ for the second lattice Boltzmann boundary scheme (33). Parameters $\alpha = -2, \beta = 1$ with \blacksquare symbol, parameters $\alpha = -2.5, \beta = 2.5$ with \square symbol. The boundary is experimentally located at $\Delta q = \frac{\Delta x}{2}$ for $\sigma_5\sigma_8 = \frac{3}{16}$ in the first case and $\sigma_5\sigma_8 = \frac{3}{8}$ in the second, as suggested in Proposition 4.

Proposition 4. For the D2Q9 lattice Boltzmann scheme (1) (26) (27) (33), the bounce-back numerical boundary condition at the wall (31) is of order 3 at location $\Delta q = \frac{\Delta x}{2}$ for the Dirichlet boundary condition $\mathbf{u} = 0$ if and only if $\sigma_5\sigma_8 = -\frac{3}{8} \frac{\alpha+4}{\alpha+2\beta-4}$.

Proof. In this case we perform the same proof as for Proposition 3, we take $F_x = 0$ and the exact solution is given by a linear longitudinal profile for density and a parabolic transverse profile for longitudinal momentum. the algebra then follows what is presented for Proposition 3. \square

We then perform simulations of the two situations discussed above. For this we consider a domain of size $N_x = 100, N_y = 21$ and analyze the flow in the steady state. For several values of σ_5 and of σ_8 , we determine a parabola by best fit with the velocity profile in the middle section of the channel. We verified that the domain was long enough in order to reduce to a negligible level the errors due to mismatch in the end boundary conditions for links that intersect both a solid boundary (imposed flux) and the input boundary (imposed pressure), that would require a more sophisticated treatment.

As in relation (10), we define Δq as the experimental point where the parabola goes through zero. The results (Fig. 4) depend only upon the product $\sigma_5\sigma_8$ and are coherent with the theoretical results established in Propositions 3 and 4. For $\alpha = -2$ and $\beta = 1$, the superconvergent accuracy is obtained “experimentally exactly” at the boundary for $\sigma_5\sigma_8 = \frac{3}{16}$. When $\alpha = -\beta = -\frac{5}{2}$, the same observation occurs for $\sigma_5\sigma_8 = \frac{3}{8}$.

5. Conclusion

The “magic” parameters introduced by Ginzburg and Adler [20] which allow to increase the accuracy of lattice Boltzmann simulations in the presence of solid boundaries have been considered for a few simple situations. We have shown that they depend upon the choice of moments and of their equilibrium values. In addition they depend upon the way the flow is driven. The analysis requires the determination of the nonequilibrium moments up to second order accuracy and this explicit form is obtained in the framework of the Taylor expansion method. Note that the same results could be obtained with the Chapman–Enskog procedure. The work described here can easily be extended to more complicated lattice Boltzmann schemes for boundaries parallel to one of the velocities of the model. In all cases that we considered, the results can be expressed in terms of products of the type $\sigma_i\sigma_j$, where σ_i corresponds to the relevant transport coefficient (diffusivity or shear viscosity) and σ_j to other moments of opposite symmetry (i.e. odd order moments of f , “energy flux” and higher order terms of the same symmetry for models with a large enough number of velocities), and thus the “magic” conditions are the same as those presented in the comprehensive paper of Ginzburg, Verhaeghe and d’Humières [24]. They are also valid for special BGK situations that we have in addition to the “magic” conditions, $\sigma_i = \sigma_j$.

Acknowledgments

The referees conveyed to the authors very interesting remarks that have been incorporated into the present edition of the article.

References

- [1] U. Frisch, D. d'Humières, B. Hasslacher, P. Lallemand, Y. Pomeau, J.-P. Rivet, Lattice gas hydrodynamics in two and three dimensions, *Complex Systems* 1 (1987) 649–707.
- [2] F. Higuera, J. Jiménez, Boltzmann approach to lattice gas simulations, *Europhysics Letters* 9 (1989) 663–668.
- [3] F. Higuera, S. Succi, R. Benzi, Lattice gas dynamics with enhanced collisions, *Europhysics Letters* 9 (4) (1989) 345–349.
- [4] Y.H. Qian, D. d'Humières, P. Lallemand, Lattice BGK models for Navier–Stokes equation, *Europhysics Letters* 17 (1992) 479–484.
- [5] D. d'Humières, Generalized Lattice-Boltzmann equations, in: *Rarefied Gas Dynamics: Theory and Simulations*, AIAA Progress in Astronautics and Astronautics 159 (1992) 450–458.
- [6] I.V. Karlin, A.N. Gorban, S. Succi, V. Boffi, Maximum entropy principle for lattice kinetic equations, *Physical Review Letters* 81 (1998) 6–9.
- [7] P. Lallemand, L. Luo, Theory of the lattice Boltzmann method: Dispersion, dissipation, isotropy, Galilean invariance, and stability, *Physical Review E* 61 (2000) 6546–6562.
- [8] P. Asinari, T. Ohwada, Connection between kinetic methods for fluid-dynamic equations and macroscopic finite-difference schemes, *Computers and Mathematics with Applications* 58 (5) (2009) 841–861, doi:10.1016/j.camwa.2009.02.009.
- [9] M. Junk, A. Klar, L.-S. Luo, Asymptotic analysis of the lattice Boltzmann equation, *Journal of Computational Physics* 210 (2005) 676–704.
- [10] F. Dubois, Une introduction au schéma de Boltzmann sur réseau, *ESAIM: Proceedings* 18 (2007) 181–215.
- [11] F. Dubois, Equivalent partial differential equations of a lattice Boltzmann scheme, *Computers and Mathematics with Applications* 55 (2008) 1141–1149.
- [12] A. Lerat, R. Peyret, Noncentered schemes and shock propagation problems, *Computers and Fluids* 2 (1974) 35–52.
- [13] R.F. Warming, B.J. Hyett, The modified equation approach to the stability and accuracy analysis of finite difference methods, *Journal of Computational Physics* 14 (1975) 159–179.
- [14] F.R. Villatoro, J.I. Ramos, On the method of modified equations. V: Asymptotic analysis of and direct-correction and asymptotic successive-correction techniques for the implicit midpoint method, *Applied Mathematics and Computation* 103 (1999) 241–285.
- [15] F. Dubois, Third order equivalent equation of lattice Boltzmann scheme, *Discrete and Continuous Dynamical Systems-Series A* 23 (2009) 221–248.
- [16] M. Junk, W.-A. Yong, Weighted L^2 stability of the lattice Boltzmann method, *SIAM Journal on Numerical Analysis* 47 (2009) 1651–1665.
- [17] M. Junk, Z. Yang, Convergence of Lattice Boltzmann methods for Navier–Stokes flows in periodic and bounded domains, *Numerische Mathematik* 112 (2009) 65–87.
- [18] D. Griffiths, J. Sanz-Serna, On the scope of the method of modified equations, *SIAM Journal on Scientific and Statistical Computing* 7 (1986) 994–1008.
- [19] S.C. Chang, A critical analysis of the modified equation technique of Warming and Hyett, *Journal of Computational Physics* 86 (1990) 107–126.
- [20] I. Ginzbourg, P.M. Adler, Boundary flow condition analysis for three-dimensional lattice Boltzmann model, *Journal of Physics II France* 4 (1994) 191–214.
- [21] I. Ginzburg, D. d'Humières, Second order boundary method for Lattice Boltzmann model, *Journal of Statistical Physics* 84 (1995) 927–971.
- [22] F. Dubois, P. Lallemand, M.M. Tekitek, Using the lattice boltzmann scheme for anisotropic diffusion problems, in: R. Eymard, J.M. Hérard (Eds.), *Finite Volumes for complex Applications V*, Wiley, 2008, pp. 351–358.
- [23] I. Ginzburg, D. d'Humières, Multireflection boundary conditions for lattice Boltzmann models, *Physical Review E* 68 (2003) 66614–66644.
- [24] I. Ginzburg, F. Verhaeghe, D. d'Humières, Two-relaxation-time lattice Boltzmann scheme: About parametrization, velocity, pressure and mixed boundary conditions, *Communications in Computational Physics* 3 (2008) 519–581.
- [25] I. Ginzburg, Generic boundary conditions for lattice Boltzmann models and their application to advection and anisotropic dispersion equations, *Advances in Water Resources* 28 (2005) 1196–1216.